Tests of Time-Reversal Invariance in Atoms, Molecules, and the Neutron

L. R. HUNTER

Sensitive experiments have been developed that search for electric dipole moments of atoms, molecules, and the neutron. These experiments play an important role in deciding which of the myriad theoretical models correctly describes violations of the principle of time-reversal invariance.

THE AESTHETIC OF SYMMETRY HAS ALWAYS PLAYED A GUIDing role in the evolution of scientific thought. The idea that the fundamental forces of nature should satisfy certain discrete symmetries is, however, a relatively recent development. In 1950 all fundamental interactions were believed to be invariant under spatial inversion (parity, P), temporal inversion (time reversal, T), and the replacement of all particles by their antiparticles (charge conjugation, C). Although the strong, electromagnetic, and gravitational forces have not yet revealed any violations of these symmetries, the weak force, which is responsible for nuclear β decay, is known to violate P maximally. Only one fundamental system in all of nature is known to violate T invariance. This violation remains one of the most intriguing mysteries in physics. T nonconservation has profound implications for our models of the fundamental constituents and interactions of nature.

The first crack in the edifice of perfect symmetry occurred in 1956, when Lee and Yang made their Nobel Prize–winning suggestion that the symmetry of P might be violated in the weak interactions (*1*). Their suggestion was quickly confirmed by the observation of an asymmetry in the β emission of polarized ^{60}Co by Wu and collaborators (*2*). This P violation is now understood as being due to the charged weak interaction, which is carried by the W boson. A P-violating neutral weak interaction, carried by the Z boson, was predicted in the late 1960s by the unified electro-weak theory of Glashow, Weinberg, and Salam (*3*). In 1974, Bouchiat and Bouchiat pointed out that this neutral weak interaction would lead to potentially observable violations of P on forbidden transitions in heavy atomic systems (*4*). A number of experiments observed this atomic P violation. These atomic experiments, along with neutrino and polarized electron–scattering experiments, confirmed the existence of the Z boson before it could actually be created at particle accelerators. A thorough review of atomic P violation has been written by Bouchiat and Pottier (*5*). Continuation of this work, especially by the group at Boulder, provides increasingly stringent tests of models of P violation and of the standard model (*6*).

After the first observation of P violation, scientists generally held that the symmetry of T invariance would continue to be conserved. In 1964, however, Christenson and colleagues (*7*) discovered that the neutral K meson system was not invariant on the combined operations of C and P. The general and powerful CPT theorem requires that a system be invariant under the combined operations of C, P, and T. From this theorem and the observed CP violation, it was concluded that the K meson system violates T invariance. Fitch and Cronin received the 1980 Nobel Prize for this first observation of T nonconservation.

The discovery of a violation of T sparked intense theoretical and experimental interest. It soon became apparent that there were several theoretical models that could account for the observed T violation and that the only way to determine which of these models was correct would be through further experimentation. A large number of experimental searches for T violation were initiated. Some of the most sensitive of these experiments look for a permanent electric dipole moment (EDM) of the neutron, atoms, and molecules. After more than a quarter-century of effort, physicists have achieved improvement of many orders of magnitude in experimental sensitivity, yet no new violation of T has been observed.

To see the connection between T invariance and a permanent EDM of a fundamental particle, consider the simple spin-1/2 particle (such as an electron or neutron) sketched in Fig. 1A. If a permanent EDM of **d** exists for this particle, it must lie along the axis of the angular momentum (*8*). Now if we imagine time to be reversed, the image of our particle will be modified as sketched in Fig. 1B. The angular momentum will reverse, but the EDM will remain fixed. Figure 1C is a 180° rotation of Fig. 1B. By comparison of Fig. 1, A and C, it becomes evident that the EDM **d** must be equal to its opposite if our system is not to violate T; that is, **d** must be zero. The principle of T invariance thus requires that the EDM of a fundamental particle be zero (*9*). The existence of a nonzero permanent EDM then implies a violation of T. A similar argument demonstrates that a nonzero EDM also implies a violation of P.

How does one go about looking for a permanent EDM? All the present methods rely in some way on a single idea: If a permanent EDM exists, then the application of an electric field perpendicular to the axis of the EDM (and hence perpendicular to the angular momentum) will result in a torque on the particle or system (Fig. 2). In a manner completely analogous to Larmor precession in a magnetic field, this electric field–induced torque results in a precession of the angular momentum about the axis of the applied electric field **E**. (In a quantum mechanical description, this precession frequency multiplied by Plank's constant, h, is simply the energy difference between adjacent magnetic sublevels.) In most experiments one searches for a small frequency shift in the Larmor precession of a system when **E** is either parallel or antiparallel to an applied magnetic field **B**. One may write the change in the precession frequency on reversal of **E** as $\Delta\nu = 2dE/L$, where L is the total angular momentum of the particle or system being studied. Thus the measurement of such a frequency change constitutes a measurement of the EDM of the particle or system of interest. The methods for measuring $\Delta\nu$ are quite different in the various experiments.

The author is Associate Professor of Physics at Amherst College, Amherst, MA 01002.

Neutron EDM Experiments

The first search for a neutron EDM, performed in 1951 by Smith Purcell, and Ramsey (*10*), was published in 1957 in response to the discovery of P violation. The neutron experiments, as well as most of early atomic experiments, were performed with some variation of the Ramsey technique of separated oscillating fields (*11*). An introduction to this technique was presented by Ramsey on his acceptance of the 1989 Nobel Prize (*12*). In this technique, a beam of particles is polarized. The polarization is rotated by a radio-frequency (RF) pulse and then precesses about parallel electric and magnetic fields. The precession is sensitively monitored by the application of a second RF pulse, phase coherent with the first, and subsequent analysis of the particles' polarization. The neutron experiments have been consistently refined since the first measurement, resulting in an improvement in sensitivity of nearly six orders of magnitude. Reviews of the early neutron experiments have been presented by Heckel (*13*) and Ramsey (*14*).

Although the early neutron experiments were all performed in beams, the most recent experiments on the neutron EDM achieve their high sensitivity by storing the neutrons in "neutron bottles." These bottles are made possible by the fact that slow neutrons can be totally internally reflected from appropriate surfaces. The Ramsey method can then be applied with the RF pulses separated by a delay time rather than by having two separate regions, as for the beam experiments. The principal advantage is that the spins have a much longer time to interact with the electric field between their "preparation" and "interrogation." The longer they have to interact, the larger the precession angle and the greater the sensitivity.

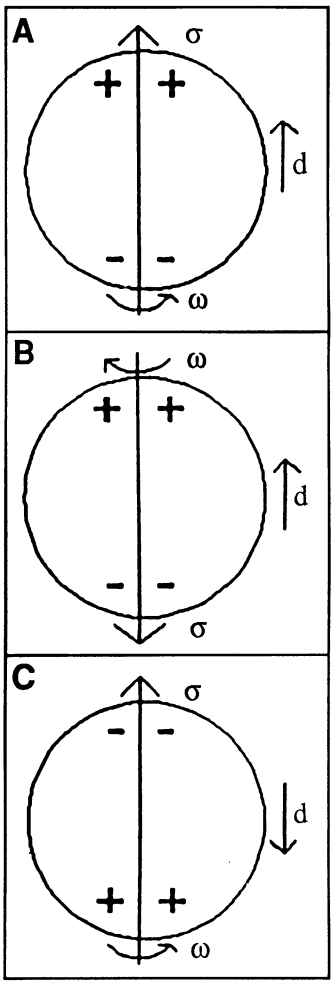

Fig. 1. T invariance implies $d = 0$. (**A**) Original particle; (**B**) time reversal of (A); (**C**) 180° rotation of (B).

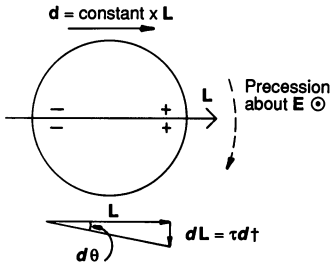

Fig. 2. The principle of all EDM measurements. An electric field **E** (directed out of the page) produces a torque $\boldsymbol{\tau} = \mathbf{d} \times \mathbf{E}$ perpendicular to **d** and **E**. Because $\tau = d\mathbf{L}/dt$, this produces a precession of the angular momentum **L** about **E** at an angular frequency

$$\omega = \frac{d\theta}{dt} = \frac{dL}{Ldt} = \frac{\tau}{L} = \frac{dE}{L}$$

For a spin-1/2 particle with $L = \hbar/2$, the precession frequency is then $\nu = 2dE/h$ ($\hbar$ is Planck's constant divided by 2π).

Two research reactors, one at Grenoble and another in Gatchina, near Leningrad, are capable of producing adequate fluxes of ultracold neutrons to fill such bottles. Ultracold neutrons (velocity $v < 7$ m/s) from the reactor are polarized as they pass through magnetically saturated Fe-Co foils. These polarized neutrons enter storage bottles with their spins aligned along a static magnetic field. A $\pi/2$ RF pulse is applied, rotating the neutron spins into a direction perpendicular to the magnetic and electric fields (~10 to 16 kV/cm). The neutrons are allowed to precess for about 50 s (Gatchina) or about 70 s (Grenoble) before a second $\pi/2$ RF pulse, coherent with the initial pulse, is applied. The bottle shutter is then opened, and the neutron polarization is analyzed as the neutrons diffuse out of the bottle through Fe-Co foils. The neutron polarization as a function of the applied RF displays the usual Ramsey double-resonance fringes (Fig. 3). To obtain maximum sensitivity, the RF is tuned to a sharp slope of the central fringe. A small change in the neutron polarization when the electric field direction is reversed ($E_{\mathrm{Up}} \rightarrow E_{\mathrm{Down}}$) yields a measurement of $\Delta\nu$ for the neutron and hence of the neutron EDM.

Any change in the magnetic field in the above experiment between the measurements made with E_{Up} and E_{Down} will result in a spurious value of $\Delta\nu$. If this change is random, it will result in magnetic noise; if it is correlated with the electric field reversal, it will result in a signal that could mimic that of the EDM. These are important concerns in nearly all EDM experiments. As a consequence, extensive magnetic shielding and magnetic field monitors, as well as great care with respect to currents induced by the voltage applied to create E, are common to most EDM experiments. In the case of the neutron experiments, five layers of high-permeability magnetic shielding and Rb (Grenoble) or Cs (Gatchina) magnetometers are used. In addition, the Soviet experiment uses two separate interaction regions: one with E_{Up} and the second with E_{Down}. These interaction volumes are separated only by the common high-voltage electrode that forms the bottom of the upper region and the top of the lower region. The regions thus will have the same magnetic precessions (to the extent that the magnetic field fluctuations are spatially homogeneous over the volume). Taking the difference between the $\Delta\nu$ observed in these two regions doubles the size of the EDM signal and reduces magnetic noise. It has the unfortunate feature of doubling the number of polarizers and analyzers one must employ. This same technique of using more than one interaction region with opposed electric fields is also used in all the atomic EDM experiments in cells.

The most recent results from these experiments are $d_{\mathrm{N}} = (-14 \pm 6) \times 10^{-26}$ e-cm (Gatchina) (*15*) and $d_{\mathrm{N}} = (-3 \pm 5) \times 10^{-26}$ e-cm (Grenoble) (*16*), where e is the charge of the electron and d_{N} is the dipole moment of the neutron. In the Gatchina experiment, a systematic discrepancy was observed between the size of the EDM measured in the two different interaction volumes. Because of this discrepancy, the authors interpret their apparently nonzero value as an upper bound on the size of the neutron EDM.

Both neutron experiments anticipate significant improvements in the future. In Gatchina, a new reactor is under construction that should produce ultracold neutron fluxes comparable to those now possible at the Grenoble reactor. In Grenoble, larger neutron bottles should provide an improvement of about a factor of 4 in the counting statistics. At present, however, the dominant problem is the ability to know precisely what magnetic field is experienced by the neutrons. This problem will become more acute as the size of the neutron interaction volumes increases. The envisioned solution involves placing an atomic magnetometer, probably ^{199}Hg but possibly ^{3}He, in the interaction chamber along with the neutrons. A number of technical problems must be overcome before this approach can succeed. The most difficult problem for the moment is finding a wall coating that will allow long spin relaxation times for both ^{199}Hg and the neutrons. Recent work suggests that a deuterated polystyrene surface may be the solution.

Atomic EDM

Measurements of atomic EDMs divide historically into two groups (*17*). The first series of measurements, performed in the 1960s, was dominated by atomic beam measurements that employed the Ramsey technique of separated oscillating fields. A hiatus occurred during the 1970s while many groups focused their attention on the pressing question of atomic P violation. A rebirth of interest in atomic EDM experiments was then triggered by the Seattle measurement of the Xe EDM in a vapor cell that demonstrated that one really could do much better (*18*). We are presently in the midst of this renaissance.

The early atomic EDM experiments. The first reported atomic EDM experiment was conducted in a pair of wall-coated cells of ^{85}Rb vapor by Ensberg at the University of Washington in 1962 (*19*). Magnetic resonance between the ground-state Zeeman levels was observed in the presence of an applied ±2 kV/cm electric field parallel to the earth's magnetic field. The cells were optically pumped with a Rb lamp and operated as Dehmelt oscillators on the basis of the principle of light modulation by precessing atoms (*20*). The difference of the oscillator frequencies between the two cells was measured to reduce the effect of fluctuations in the earth's magnetic field. This frequency difference was found to be unchanged on the reversal of the direction of **E**. From this experiment the author concluded that $|d_{Rb}| < 10^{-18}$ e-cm.

With the exception of this first measurement, all the early atomic experiments were performed in atomic beams. The first atomic beam experiment designed to test for a permanent EDM of an atom was conducted at Brandeis in 1964 (*21*). This experiment used the Ramsey separated oscillating field technique to measure the splitting between the $m_F = 4$ and $m_F = 3$ magnetic substates of the $F = 4$ hyperfine level of the Cs ground state. The authors searched for a change in this splitting when the applied electric field **E** was either parallel or antiparallel to a magnetic field **B**. The upper bound on the Cs EDM obtained by this method was about 2×10^{-19} e-cm.

This early experiment was limited by an inability to align **E** and **B** precisely parallel to each other. In the atom's rest frame a motional magnetic field, $\mathbf{B}_{mot} = -\mathbf{v}/c \times \mathbf{E}$, is produced by the applied **E**. Any misalignment between **B** and **E** can then result in a change in the total **B** and hence in the observed Zeeman frequency. This frequency change would clearly change sign with the reversal of **E**, precisely imitating the signature of the atomic EDM. Subsequent experiments addressed this problem by introducing a lighter atom, expected to have a much smaller EDM (*22*), as a magnetic field monitor. These experiments on Cs (*23*), Tl (*24*), and metastable Xe (Xe*) (*25*) resulted in an improvement of about three orders of magnitude over the previous best limits on an atomic EDM.

Atomic EDM experiments, the next generation. The present generation of atomic EDM experiments was initiated in the early 1980s. The new experiments employ various novel techniques but have a few common features. All these experiments rely on optical pumping for state preparation and on some form of optical detection scheme. These optical schemes are both more efficient and intrinsically less noisy than the magnetic techniques used in earlier work. With the exception of the Hg experiment, all these experiments were made possible or easier by the development of new laser sources during the previous decade.

Xenon. The experiment to measure the ^{129}Xe ground-state EDM demonstrated that atomic EDMs could be measured several orders of magnitude more accurately than had previously been possible. The experiment relied on some elegant optical pumping techniques that were developed during the 1970s. Rubidium, placed in the cells along with Xe, is oriented by illumination of the cells with circularly polarized light from a single-mode diode laser tuned to the Rb D1 resonance. A magnetic field, parallel to the light-propagation direction **k**, is applied during the pumping to maintain the polarization direction. The Xe is polarized along **k** through spin exchange with the Rb. After a sufficient polarization of the Xe nucleus is achieved, the magnetic field along **k** is removed and replaced by parallel **E** (~4.5 kV/cm) and **B** (~0.1 mG) fields that are perpendicular to **k**. The Xe spins precess freely about the applied fields, producing a rotating Xe magnetization. The Xe polarization is transferred by spin exchange back to the Rb. An oscillating magnetic field is applied perpendicular to both **B** and **k** to produce a modulation in the Rb polarization. Synchronous detection of the transmission of the circularly polarized light at this modulation frequency yields a signal that reflects the net Rb polarization direction and hence indirectly the Xe magnetization. The Xe precession frequency can be measured accurately because the coherence relaxation time for the Xe in these cells with 220 torr of nitrogen buffer gas is about 500 seconds. One searches for a change in this precession frequency when the **E** field is either parallel or antiparallel to **B**. A stack of three cells is used to reduce any effects associated with changes in the

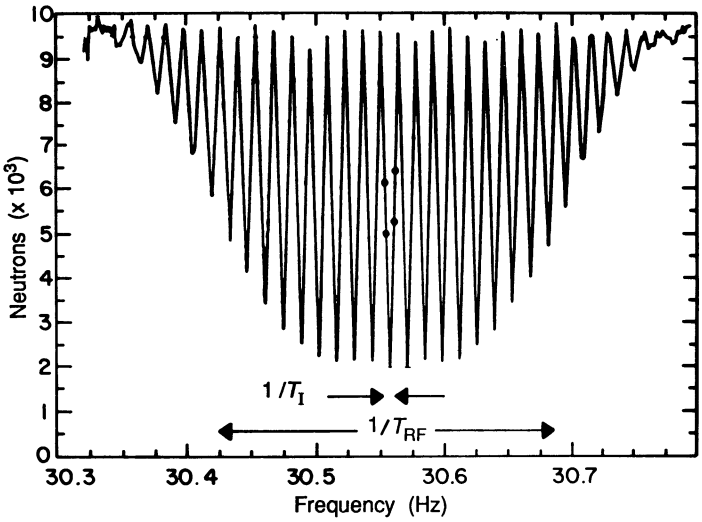

Fig. 3. A resonance curve obtained for neutrons by means of the separated oscillatory fields technique. The width of the envelope of the curve is proportional to $1/T_{RF}$, where T_{RF} is the time of interaction with the phase-coherent RF pulses. The width of the fringes is proportional to $1/T_I$ where T_I is the time between the two RF pulses (when the particles interact with the static **E** and **B** fields). T_I can be made very long, resulting in sharp fringes and hence good frequency resolution. The four points indicate the frequencies at which the experiment was conducted. (Data provided by S. Lamoreaux.)

ambient **B** field. Because the atoms are confined to a cell, motional field effects are expected to be small. With all these advantages, the EDM of Xe was measured to be $d_{Xe} = (-0.3 \pm 1.1) \times 10^{-26}$ e-cm, an improvement of more than four orders of magnitude over any previous atomic EDM measurement.

Mercury. On completion of the Xe experiment, the Seattle group realized that if they could obtain comparable limits on the ground state of Hg they would be able to achieve an order of magnitude improvement in their sensitivity to most T-violating interactions (an atom's sensitivity to fundamental T-nonconserving processes rises rapidly with atomic number). With this in mind, they began an experiment to measure the Hg EDM (*26*). In this experiment the Hg was optically pumped by 253.7-nm light from a Hg discharge lamp. Two cells were operated as light-absorption oscillators based on the Larmor precession frequency of ^{199}Hg. Circularly polarized light propagates through the cells along **k**. **E** is again perpendicular to **k**, but the static magnetic field $\mathbf{B}_o$ makes a 45° angle relative to both **k** and **E**. The oscillatory magnetic field $\mathbf{B}_x$ remains perpendicular to both **k** and $\mathbf{B}_o$ and oscillates at frequency ω close to the Larmor frequency ω_o. The nuclear polarization is then driven by the oscillating field to precess in a cone about $\mathbf{B}_o$ with a frequency ω, modulating the intensity of the transmitted light at the same frequency. For $\omega = \omega_o$ the light modulation will be exactly in phase with $\mathbf{B}_x$, whereas for small deviations from equality there will be a phase shift $\phi = T_2(\omega - \omega_o)$, where T_2 is the transverse relaxation time of the polarization. By using a stack of two cells with their electric fields opposed, the average phase shift may be kept close to zero by adjusting $\mathbf{B}_o$. A change in the difference of ϕ between the two cells on reversal of **E** constitutes a measurement of the Hg EDM. With this arrangement, the Seattle group achieved the result $d_{Hg} = (0.7 \pm 1.5) \times 10^{-26}$ e-cm. At the time of its publication, this result placed the most stringent limits on nearly all the T-violating processes expected to play a role in atomic systems.

A new version of this experiment that uses an improved optical pumping geometry (*27*) is now in progress and has already produced initial results with an improvement of nearly a factor of 10 in the experimental signal-to-noise ratio. The addition of a small amount of carbon monoxide to the cells to trap oxygen has increased the cells' usable lifetimes, permitting much longer integration times. With these improvements, a statistical precision of $10^{-27}e$-cm has been achieved. The authors are now investigating possible systematic uncertainties.

Cesium. Although the atomic limits in Xe and Hg are impressive (because neither atom has an unpaired electron), the bounds one can place on the electron EDM are in fact just competitive with the earlier atomic beam measurements. When I heard of Fortson's success with Xe, I wondered whether it would be possible to use some of the intrinsic advantages of the cell environment (high density, long relaxation times, and small motional field effects) with a paramagnetic atom to improve the bounds on the electron EDM. The method I proposed, unlike all previous methods used to measure atomic EDMs, does not require the application of any magnetic field during data acquisition. The first version of this experiment has been completed successfully (*28*).

Light from a circularly polarized single-mode diode laser (894 nm), propagating along **x**, excites the $6S_{1/2}$ ($F = 3$) $\rightarrow$ $6P_{1/2}$ transition in Cs in the presence of a 4 kV/cm electric field (along **z**). Optical pumping, spin exchange, and polarization transfer through the excited state create an orientation of the $6S_{1/2}$ ($F = 4$) level along **x**. Long spin relaxation times (~16 msec) are achieved by adding 250 torr of nitrogen as a buffer gas.

If Cs has a permanent EDM, the applied **E** field will create a torque on the oriented Cs atoms that causes the ground-state polarization to precess into the **y** direction. To detect this polarization a second diode laser beam, propagating along **y** and tuned to the $6S_{1/2}$ ($F = 4$) to $6P_{1/2}$ transition, probes the Cs vapor. The circular polarization of this second laser is rapidly modulated between right and left by a photoelastic modulator. The transmission of this probe beam through the vapor is detected synchronously with the circular polarization reversal by a lock-in detector, the output of which is proportional to the atomic polarization along **y**. If **E** is reversed, the sign of the EDM-induced polarization must also reverse. The effect is exactly analogous to the Hanle effect (*29*), with the magnetic Hamiltonian $\boldsymbol{\mu} \cdot \mathbf{B}$ being replaced by the electric Hamiltonian $\mathbf{d} \cdot \mathbf{E}$.

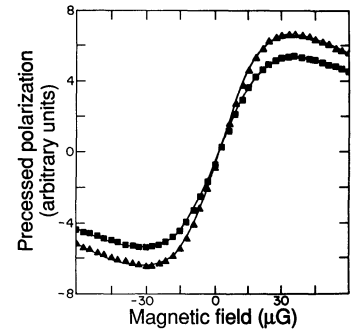

Fig. 4. Experimentally observed Hanle curve for initial polarization along **x** and magnetic field along **z**. The resulting polarization is observed along **y**. (Cell 1, ■; cell 2, ▲).

Great care is taken to eliminate magnetic fields from the experiment. An array of passive and active magnetic shields allows all three components of the residual magnetic field in the cells to be maintained below 100 nG. Taking the difference in the polarization signals obtained from two stacked cells with opposed electric fields doubles the size of the EDM signal while canceling rotations induced by the residual magnetic field (to the extent that **B** is the same in the two cells). The EDM polarization, in addition to being of opposite sign in the two cells, is required to change sign on reversal of the incident circular polarization, the probe circular polarization, and the applied high voltage. This highly specific signature allows many possible systematic effects to be distinguished that might otherwise mimic the EDM signal. The experimental sensitivity is calibrated by applying a known magnetic field and observing the change in the lock-in signals for each cell. A typical Hanle curve obtained for the Cs ground state is shown in Fig. 4. Because d_{Cs} is small, only the slope of the curves near $\mathbf{B} = 0$ is required for calibration.

With this simple and relatively inexpensive method, investigators have measured the Cs EDM to be $d_{Cs} = (-1.8 \pm 6.9) \times 10^{-24}$ e-cm. This result represents an improvement of a factor of 25 over the earlier Cs experiment performed in an atomic beam. Investigators are now working to achieve yet another order of magnitude increase in sensitivity. A factor of 4 improvement in the signal-to-noise ratio is anticipated by increasing the Cs vapor pressure. New cells have been designed with recessed electrodes that allow a reduction in systematic uncertainties associated with leakage currents to an insignificant level. Two new cells have been added, above and below the usual pair of cells, as Cs magnetometers. This configuration enables the noise associated with fluctuations in the gradient of the magnetic field at the cells to be removed. In addition, new methods of polarization analysis are being explored. The mechanical stability of the apparatus has been improved so that longer integration times can be achieved. The net result of these changes should be an order of magnitude improvement in sensitivity.

More long-term methods of improving the Cs EDM measurement are also being investigated. One possibility involves the use of the nonlinear Faraday effect on the $6S_{1/2}$–$6P_{1/2}$ transition, which recently was observed for the first time. With the use of a multipass

Table 1. Best limits on T violation from EDM measurements. Quoted uncertainties are quadratic sums of the statistical and systematic uncertainties. Theoretical uncertainties discussed in the text have not been included.

Measurement	Xe (1984)	Hg (1987)	Cs (1989)	TlF (1989)	Tl (1990)
Atomic EDM (10^{-25} e-cm)	-0.03 ± 0.11	0.07 ± 0.15	-18 ± 69	(-130 ± 220) μHz*	16 ± 50
Electron EDM (10^{-26} e-cm)	400 ± 1400	-50 ± 110	-2 ± 6	-12 ± 35	-0.3 ± 0.8
Proton EDM (10^{-23} e-cm)	-70 ± 260		-230 ± 880	-4 ± 6	
Schiff moment (10^{-23} e-cm-fm^2)	-9 ± 32	-2 ± 4		-2 ± 4	
e-N tensor coupling (10^{-7} G_F)	6 ± 21	-1 ± 3		-2 ± 3	
e-N scalar coupling (10^{-6} G_F)	80 ± 290	10 ± 22	3 ± 10	6 ± 10	0.3 ± 1.0

*The molecular results are most conveniently expressed in terms of the frequency D/h.

cell in an appropriate geometry, this method may yield an even more sensitive method for determining the Cs EDM. Slowed Cs atoms in something like an "atomic funnel" or "fountain" may eventually provide even further improvement (*30, 31*). The ease of optically cooling and manipulating Cs make it an excellent candidate for such experiments.

Thallium. A new atomic beam experiment in Berkeley on ^{205}Tl has several innovative features that have already allowed a factor of 500 improvement on the previous Tl EDM limits (*32*). The experiment makes use of the separated oscillating field magnetic resonance method, but the magnetic-state selection has been replaced by a more efficient optical pumping arrangement with 378-nm light generated by an intracavity doubled-ring dye laser. The light, linearly polarized along z, excites the $6^2P_{1/2}$ $(F = 1) \rightarrow 7^2S_{1/2}$ $(F = 1)$ transition. Although both the $m_F = +1$ and -1 levels of $F = 1$ will be excited, the $6P_{1/2}$ $(F = 1, m_F = 0) \rightarrow 7S_{1/2}$ $(F = 1, m_F = 0)$ matrix element is zero. After a sufficient number of excitation cycles the populations of the ground-state $m_F = \pm 1$ are thoroughly depleted, whereas the population of the $m_F = 0$ level is enhanced. After this optical-state selection, the Tl beam passes through the usual RF and static field regions. An electric field of 100 kV/cm and a magnetic field of 0.26 G are applied in the central 1-m-long region. The second RF region is followed by an optical excitation region identical to that used for state preparation. Ellipsoid reflectors focus the 535-nm fluorescent light from the $7S_{1/2} \rightarrow 6P_{3/2}$ transition onto appropriate photomultipliers. If, after traversing the RF and static field regions, the atoms have returned to the $m_F = 0$ level of $6P_{1/2}$, no fluorescence will be detected. Any transitions to $m_F = \pm 1$ level will be detected through the subsequent decay fluorescence. The fluorescence signal will thus exhibit a Ramsey fringe pattern as the RF is varied, and the usual techniques for measuring the atomic EDM may then be employed.

The Berkeley group has developed an effective means of minimizing the uncertainties associated with motional field effects. They simply reverse the direction of the atomic beam, thereby changing the sign of $\mathbf{v} \times \mathbf{E}$ but leaving the EDM signal unaltered. To accomplish this, their apparatus has been constructed to be longitudinally symmetric about the center of the atomic beam. Their atomic beam is oriented vertically to ensure that the trajectories of atoms with differing velocities are identical. The state preparation and analysis regions are identical, as are the ovens on the top and bottom of the apparatus. This symmetry allows the propagation direction of the atomic beam to be reversed with the simple insertion or removal of appropriate beam stops. The alignment between the **E** and **B** fields can then be carefully adjusted to eliminate the $\mathbf{v} \times \mathbf{E}$ effects. The most recent result from this experiment is $d_{Tl} = (1.6 \pm 5.0) \times 10^{-24}$ e-cm.

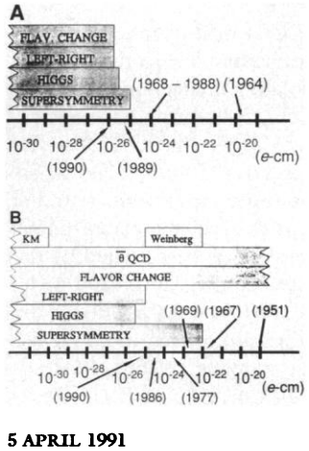

Fig. 5. Predictions of various theoretical models for (**A**) electron and (**B**) neutron EDMs. The experimental limits of various years are labeled.

Molecular EDM: Thallium Fluoride

One often speaks of a molecule as having a dipole moment along its internuclear axis. Such a concept, although useful for discussing the behavior of a molecule in a strong electric field, is, strictly speaking, not correct. In the weak field limit, the energy level shift induced by an external electric field on a molecule increases quadratically and not linearly with the field. A polar molecule thus has no permanent EDM unless there is a violation of T.

In 1967, Sandars noted that the TlF molecule provides a sensitive testing ground for fundamental processes that violate T (*33*). From perturbation theory we know that the mixing of states induced by any T-violating process will be proportional to the strength of the T-violating Hamiltonian divided by the energy difference between the levels to be mixed. In a molecule, T-violating processes can mix adjacent rotational levels. Because the spacing between these levels is much smaller than that between electronic energy levels in an atom, the size of the mixing induced can be greatly enhanced. Stimulated by this observation, a long and relatively continuous series of EDM experiments was conducted on the TlF molecule. These experiments were begun in Oxford (*34, 35*), were continued at Harvard (*36*), and have now reached their most sophisticated level at Yale (*37, 38*).

The TlF experiments all search for an interaction Hamiltonian H that depends on the relative orientation of the spin-1/2 Tl nucleus ($\boldsymbol{\sigma}$) and the internuclear axis of the molecule ($\boldsymbol{\lambda}$). An interaction of the form $H = -D\boldsymbol{\sigma} \cdot \boldsymbol{\lambda}$ (where D is a constant) would result in a permanent EDM of the TlF molecule.

In the most recent experiments, a new supersonic molecular beam source provides an intense beam of rotationally cold TlF monomers. The rotational substate ($J = 1, m_J = 0$) is focused by an electrostatic quadrupole field into a state selector where an RF field drives a transition in the presence of static electric and magnetic fields. The net result of this is the selection of a specific magnetic sublevel of the molecular system, with $\boldsymbol{\sigma}$ now being oriented along the magnetic field **B**. The polarized molecules then pass adiabatically into a region that contains only an electric field **E** (29.5 kV/cm). The nuclear magnetic resonance (NMR) transition is then induced by means of

the same separated oscillating field technique previously described. Molecules that have not undergone a spin flip are then selected and focused onto a hot wire detector. A change in this detector current with the reversal of the relative phase of the oscillating field constitutes the NMR signal. As a consequence of the improved beam source, the signal-to-noise ratio was improved by a factor of 14 over that of the previous experiment.

With this higher sensitivity and additional attention to possible systematic effects, the Yale group measured the change in the NMR frequency with the reversal of **E** to be (140 ± 240) μHz. This result reduces the limit on the EDM of the TlF molecule by an order of magnitude. Efforts to improve this experiment by another order of magnitude through the optimization of the experimental parameters are now under way. Improvement beyond this latter point will probably require the development of a method to cool the molecular beam.

Derived Limits on T Violation

If T violation is observed in an atom, it could be due to an intrinsic T violation of any of the atomic constituents (electron, proton, or neutron) or to the interactions among these constituents. Detailed theoretical models have been developed to relate the size of these potential contributions to the measured atomic EDMs (*39*). We will now examine how these fundamental sources of T violation are parameterized and what limits can be placed on them from present experiments. The uncertainties associated with this analysis also will be discussed.

The electron EDM. The intrinsic T violation of the electron is conveniently expressed in terms of d_e, the electron EDM. Naively, one might assume that an atom would be insensitive to an EDM of one of its constituents, because the atomic charge would adjust to shield the electric field that would be experienced by any individual neutron, proton, or electron. In a nonrelativistic atom with any pointlike particles bound by electrostatic forces, this is indeed the case. If we include either the strong nuclear force or relativity (or, equivalently, magnetic forces), however, then a constituent edm can give rise to an atomic EDM (*40*).

In 1965, Sandars pointed out that in heavy paramagnetic atoms the size of the atomic edm (d_A) induced by d_e can in fact exceed d_e by two to three orders of magnitude, making such an atom a sensitive probe for detecting d_e. For these atoms, the ratio $R = d_A/d_e$ is expected to scale roughly as $Z^3\alpha^2$, where α is the fine-structure constant and Z is the atomic number (*22*). Semiempirical calculations (*24, 41*) for Xe* yield the values $R_{Xe^*} = 130$ and 120. The most recent Hartree-Fock calculations for Cs and Tl yield $R_{Cs} = 114 \pm 3$ and $R_{Tl} = -600 \pm 400$ (*42–45*). The Cs result is in excellent agreement with earlier semiempirical calculations (*22, 41*). The large theoretical uncertainty quoted for R_{Tl} is a reflection of the failure of the Hartree-Fock calculations to converge when carried to higher order. In view of the consistency of earlier semiempirical calculations for Tl (*41, 46*), it is likely that the uncertainty in R_{Tl} is no larger than 30%. The smaller theoretical uncertainty in Cs is a result of its more tightly bound electronic core and clearly makes it the most desirable atom for precision measurements should an electron EDM be found.

Because Xe, Hg, and TlF have total electronic spins of zero, an electron EDM can only induce an atomic EDM in these systems through effects described by higher order perturbation theory. The process can essentially be thought of as the electron shells being polarized through their hyperfine coupling to the nuclear spin. Detailed calculations (*47*) for these systems yield the results $R_{Xe} = -0.8 \times 10^{-3}$ and $R_{Hg} = -1.4 \times 10^{-2}$. These calculations may have an uncertainty of less than 40%. A Hartree-Fock calculation confirms the Xe result but finds the Hg enhancement factor to be $R_{Hg} = 1.2 \times 10^{-2}$, which is smaller and of opposite sign (*48*). The authors of the Hartree-Fock calculation believe that higher order effects may be important in their Hg calculation and might resolve the discrepancy.

The resulting limits on the electron EDM from the most recent experiments (without theoretical uncertainties) are listed in Table 1. As an illustration of the sensitivity of the EDM limits, if an electron with a classical electron radius ($\sim 2.8 \times 10^{-13}$ cm) were blown up to the size of the earth, these EDM limits would correspond to a displacement of its center of charge from its center of mass by less than 20 μm, less than the thickness of a hair.

The nuclear EDM. The finite nuclear size makes it possible for a nuclear EDM to produce an atomic EDM. The effective Hamiltonian describing this T violation in the nucleus is usually parameterized in terms of the Schiff moment **Q** (*49*):

$$H_N = -4\pi e\mathbf{Q} \cdot \nabla\rho(0) \quad . \tag{1}$$

Q is related to the nuclear dipole distribution in the nucleus and is directed along the nuclear spin. The term $\nabla\rho(0)$ is the gradient of the electron density induced at the nucleus. Calculations of the relationship between **Q** and the various measured EDMs have been carried through for Tl (*49*), Xe (*50*), Hg (*51*), and TlF (*52*). The resulting limits are listed in Table 1.

A nuclear EDM can have as its source an EDM of the constituent nucleons or the interactions among nucleons. The limits on the neutron EDM obtained thus far from atomic experiments are not competitive with the direct measurements on the neutron. Limits on the proton EDM, extracted from the Xe and TlF measurements, are listed in Table 1. The best limits on the T-violating nucleon-nucleon weak coupling, about $10^{-2}\ G_F$ (G_F is the Fermi coupling constant), are obtained from the TlF and Hg experiments. Because of theoretical ambiguities, the limits on the proton EDM and the nucleon-nucleon weak couplings should probably be regarded as estimates only accurate to about a factor of three.

Semileptonic weak interaction. A T-violating interaction between an electron and the nucleus could also induce an atomic EDM. The weak couplings that could produce such an interaction are a tensor current coupling to a pseudotensor current

$$H_T = C_T\,(G_F/\sqrt{2})\,(\bar{e}i\gamma_5\sigma_{\mu\nu}e)\,(\bar{n}\sigma^{\mu\nu}n) \tag{2}$$

or the scalar-hadronic current coupling to the pseudoscalar electronic current

$$H_S = C_S\,(G_F/\sqrt{2})\,(\bar{e}i\gamma_5 e)\,\bar{n}n \tag{3}$$

Here e and n are the electron and nucleon field operators, respectively. The terms C_S and C_T are dimensionless constants that characterize the strengths of these T-violating interactions relative to the usual T-conserving weak interactions. Interesting limits on C_S and C_T come from Tl, Xe, Hg, TlF, and Cs (*39, 47, 48, 52, 53*). The derived limits on these couplings are listed in Table 1. The scalar-pseudoscalar interaction is to lowest order proportional to the electron spin, resulting in a higher sensitivity in the paramagnetic atoms. The tensor-pseudotensor interactions is best limited by the atoms without electron spin because the atomic limits tend to be much better in these atoms. The limits on C_S and C_T imply that the T-violating electron-nucleon couplings are at least 10^6 times smaller than the P-violating but T-conserving coupling. Nature truly appears reluctant to violate T.

Implications for Theory

How do these results compare with the predictions of various models of T violation? Most of the particle theory done thus far has focused on predictions of the EDM of the electron and neutron. In all these models the proton is anticipated to have an EDM comparable to that of the neutron. In view of the better sensitivity of the neutron experiments, it suffices to compare theory with the electron and neutron results. A summary of the EDM predictions (*54–59*) along with the experimental bounds for various years is shown in Fig. 5. It is evident that a number of models either have already been ruled out or have been constrained by experiment. Weinberg's 3-Higgs model has effectively been ruled out as a source of the K meson and neutron T violation. The sensitivity to the electron EDM is rapidly approaching the interesting level of 10^{-27} *e*-cm, where a number of models will be constrained.

Conclusions

A series of increasingly sensitive searches for permanent EDMs of neutrons, atoms, and molecules has thus far only produced upper limits on their size. Experimental techniques are evolving rapidly, and the rate of progress on these experiments is truly impressive. One or two orders of magnitude improvement in all these experiments would appear to be likely within the next few years. The next decade will certainly see the application of the rapidly improving techniques of laser cooling and confinement to the search for an atomic EDM. These experiments will probably achieve several orders of magnitude improvement over the present generation. With this increased sensitivity, it is possible that an EDM of the neutron, an atom, or a molecule could soon be observed. Such a discovery would constitute only the second violation of the principle of T invariance. Even if an EDM is not detected, this new generation of experiments will play a large role in unraveling the mystery of the origin of T nonconservation.

REFERENCES AND NOTES

1. T. D. Lee and C. N. Yang, *Phys. Rev.* **104**, 254 (1956).
2. C. S. Wu, E. Ambler, R. W. Hayward, D. D. Hoppes, R. F. Hudson, *ibid.* **105**, 1413 (1957).
3. S. L. Glashow, *Nucl. Phys.* **22**, 579 (1961); S. Weinberg, *Phys. Rev. Lett.* **19**, 1264 (1967); A. Salam, in *Elementary Particle Theory: Relativistic Groups and Analyticity*, Nobel Symposium No. 8, N. Svartholm, Ed. (Almquist and Wiksell, Stockholm, 1968).
4. M. A. Bouchiat and C. Bouchiat, *Phys. Lett. B* **48**, 111 (1974).
5. M. A. Bouchiat and L. Pottier, *Science* **234**, 1203 (1986).
6. M. C. Noecker, B. P. Masterson, C. E. Wieman, *Phys. Rev. Lett.* **61**, 310 (1988).
7. J. H. Christenson, J. Cronin, V. L. Fitch, R. Turlay, *ibid.* **13**, 138 (1964).
8. This assertion can be established by considering the Pauli principle. If the EDM of either a neutron or an electron were to lie along any axis other than that of the angular momentum, we would require a new quantum number to describe the EDM's projection along this new axis. Just as spin-up is distinguished from spin-down, we would then be able to distinguish "EDM-up" from "EDM-down" and hence would be able to construct nuclei and atoms with twice as many particles in each shell as we could without this new quantum number.
9. For a more formal and rigorous derivation see E. M. Purcell and N. F. Ramsey, *Phys. Rev.* **78**, 807 (1950).
10. J. H. Smith, E. M. Purcell, N. F. Ramsey, *ibid.* **108**, 120 (1957).
11. N. F. Ramsey, *Molecular Beams* (Clarendon, Oxford, 1963).
12. ———, *Rev. Mod. Phys.* **62**, 541 (1990).
13. B. Heckel, in *Atomic Physics Nine*, R. S. Van Dyck, Jr., and E. N. Fortson, Eds. (World Scientific, Singapore, 1984).
14. N. F. Ramsey, *Rep. Prog. Phys.* **45**, 95 (1982).
15. I. S. Altarev *et al.*, *JETP Lett.* **44**, 460 (1986).
16. K. F. Smith *et al.*, *Phys. Lett. B* **234**, 191 (1990).
17. For a review through 1988, see also E. Hinds, in *Atomic Physics No. 11*, S. Haroche, J. C. Gay, G. Grynberg, Eds. (World Scientific, Singapore, 1989).
18. T. G. Vold, F. J. Raab, B. Heckel, E. N. Fortson, *Phys. Rev. Lett.* **52**, 2229 (1984).
19. E. S. Ensberg, *Bull. Am. Phys. Soc.* **7**, 534 (1962).
20. H. G. Dehmelt, *Phys. Rev.* **105**, 1924 (1957).
21. P. G. H. Sandars and E. Lipworth, *Phys. Rev. Lett.* **13**, 718 (1964).
22. P. G. H. Sandars, *Phys. Lett.* **14**, 194 (1965); *ibid.* **22**, 290 (1966).
23. M. C. Weiscopf, J. P. Carrico, H. Gould, E. Lipworth, T. S. Stein, *Phys. Rev. Lett.* **21**, 1645 (1968).
24. H. Gould, *ibid.* **24**, 1091 (1970).
25. M. A. Player and P. G. H. Sandars, *J. Phys. B* **3**, 1620 (1970).
26. S. K. Lamoreaux, J. P. Jacobs, B. R. Heckel, F. J. Raab, N. Fortson, *Phys. Rev. Lett.* **59**, 2275 (1987).
27. S. K. Lamoreaux, *Nucl. Instrum. Methods* **A284**, 43 (1989).
28. S. A. Murthy, D. Krause, Jr., Z. L. Li, L. R. Hunter, *Phys. Rev. Lett.* **63**, 965 (1989).
29. A thorough description of the Hanle effect can be found in A. Corney, *Atomic and Laser Spectroscopy* (Clarendon Press, Oxford, 1977).
30. E. Riis, D. S. Weiss, K. A. Moler, S. Chu, *Phys. Rev. Lett.* **64**, 1658 (1990).
31. M. A. Kasevich, E. Riis, S. Chu, R. DeVoe, *ibid.* **63**, 612 (1989).
32. K. Abdullah, C. Carlberg, E. D. Commins, H. Gould, S. B. Ross, *ibid.* **65**, 2347 (1990).
33. P. G. H. Sandars, *ibid.* **19**, 1396 (1967).
34. G. E. Harrison, P. G. H. Sandars, S. J. Wright, *ibid.* **22**, 1263 (1969).
35. E. A. Hinds and P. G. H. Sandars, *Phys. Rev. A* **21**, 480 (1980).
36. D. A. Wilkening, N. F. Ramsey, D. J. Larson, *ibid.* **29**, 425 (1984).
37. D. Schropp, Jr., D. Cho, T. Vold, E. A. Hinds, *Phys. Rev. Lett.* **59**, 991 (1987).
38. D. Cho, K. Sangster, E. A. Hinds, *ibid.* **63**, 2559 (1989).
39. For a recent review see I. B. Khriplovich, in *Atomic Physics No. 11*, S. Haroche, J. C. Gay, G. Grynberg, Eds. (World Scientific, Singapore, 1989).
40. L. I. Schiff, *Phys. Rev.* **132**, 2194 (1963).
41. V. V. Flambaum, *Yad. Fiz. (Sov. J. Nucl. Phys.)* **24**, 383 (1976).
42. A. C. Hartley, E. Lindroth, A. M. Mårtensson-Pendrill, *J. Phys. B.* **23**, 3417 (1990).
43. A. Y. Kraftmakher, *ibid.* **21**, 2803 (1988).
44. W. R. Johnson, D. S. Guo, M. Idrees, J. Sapirstein, *Phys. Rev. A* **32**, 2093 (1985).
45. A. M. Mårtensson-Pendrill and P. Oster, *Phys. Scr.* **T36**, 444 (1987).
46. P. G. H. Sandars and R. M. Sternheimer, *Phys. Rev. A* **11**, 473 (1975).
47. V. V. Flambaum and I. B. Khriplovich, *Zh. Eksp. Teor. Fiz.* **89**, 1505 (1985) [*Sov. Phys. JETP* **62**, 872 (1985)].
48. A. M. Mårtensson-Pendrill, *Phys. Rev. Lett.* **54**, 1153 (1985).
49. I. B. Khriplovich, *Zh. Eksp. Teor. Fiz.* **71**, 51 (1976) [*Sov. Phys. JETP* **44**, 25 (1976)].
50. V. A. Dzuba, V. V. Flambaum, P. G. Silverstrov, *Phys. Lett. B* **154**, 93 (1985).
51. V. V. Flambaum, I. B. Khriplovich, O. P. Sushkov, *ibid.* **162**, 213 (1985); *Nucl. Phys. A* **449**, 750 (1986).
52. P. V. Coveney and P. G. H. Sandars, *J. Phys. B* **16**, 3727 (1983).
53. C. Bouchiat, *Phys. Lett. B* **57**, 284 (1975).
54. For a recent review see S. M. Barr and W. J. Marciano, in *CP Violations*, C. Jarlskog, Ed. (World Scientific, Singapore, 1989).
55. J. F. Donaghue, B. R. Holstein, G. Valencia, *Int. J. Mod. Phys. A* **2**, 319 (1987).
56. S. Weinberg, *Phys. Rev. Lett.* **63**, 2333 (1989).
57. S. M. Barr and A. Zee, *ibid.* **65**, 21 (1990).
58. R. G. Leigh, S. Paban, R.-M. Xu, *Nucl. Phys. B*, in press.
59. D. Chang, W.-Y. Keung, T. C. Yuan, *Phys. Rev. D* **43**, 14 (1991).

60. Supported by the National Science Foundation and the A. P. Sloan Foundation.